Available online at www.sciencedirect.com
ScienceDirect
Thermochimica Acta 457 (2007) 83–91
thermochimica acta
www.elsevier.com/locate/tca

Chlorination of aluminium–copper alloys

G. De Micco [a,b,*], D.M. Pasquevich [a,c], A.E. Bohé [c,d]

[a] Comisión Nacional de Energía Atómica (C.N.E.A.), Avenida Bustillo 9500, 8400 San Carlos de Bariloche, Argentina
[b] Universidad Nacional de Cuyo, Instituto Balseiro, Avenida Bustillo 9500, 8400 San Carlos de Bariloche, Argentina
[c] Consejo Nacional de Investigaciones Científicas y Técnicas (CONICET), Argentina
[d] Universidad Nacional del Comahue, Centro Regional Universitario Bariloche, 8400 San Carlos de Bariloche, Argentina

Received 22 December 2006; received in revised form 6 February 2007; accepted 16 February 2007
Available online 27 February 2007

Abstract

The chlorination of Al–Cu alloys is investigated by thermogravimetry, X-ray diffraction, scanning electron microscopy, energy dispersive spectroscopy, and energy dispersive X-ray fluorescence, between 200 and 500 °C. The starting temperature for the chlorination of selected alloys is determined. Results indicate that the reactivity of the alloys is different from that of the pure metals. Analysis of the reaction products reveals that there are interactions between the different chlorides formed. These interactions lead to an enhancement in the copper chlorides volatilization and the formation of well-developed crystals of $CuCl_2$ instead of the mixture of $CuCl_2$ and CuCl that is obtained in the chlorination of pure copper. A schematic diagram that describes the chlorination mechanisms for the pure metals and AlCu alloys is presented.

Keywords: Chlorination; Aluminium–copper alloys; Thermogravimetry

1. Introduction

The reactions of chlorine with pure metals have not been thoroughly studied. The majority of the studies are concerned with production of anhydrous chlorides for industrial applications [1–7]. Even less is the information available on alloy chlorination. However, in the last few years, an increasing number of chlorination studies related with the recovery of valuable metals such as Co, Ni, V, W, Mo, Cr, Fe, Cu, and Zn from complex scraps have been published [8–10]. This indicates that the chlorination process has become an important technological subject.

As far as basic research is concerned, Landsberg studied the chlorination rates of Si–Ge, Mo–Re and Au–Pt alloys with respect to temperature and chlorine pressure. He found that the reactivities of the alloys are different from those of the pure constituents [11]. Chang and Wei [12] reviewed the corrosion of several metals and alloys in atmospheres containing chlorine above 200 °C. Regarding kinetics and mechanism he states that high temperature corrosion consists mainly of diffusion of ions in the scale of chlorides formed and volatilization of the scale.

To the authors' best knowledge, the reaction of chlorine with Al–Cu alloys has not been studied. It is only known that the reaction of chlorine with aluminium yields $AlCl_3$ [1–5,13], while that of chlorine with copper has two possible products, CuCl and $CuCl_2$ [14]. For copper, in addition to the information related with synthesis of copper(I) chloride by dry chlorination [7,8,14], a few basic studies are available [15–18]. Recently, De Micco et al. [18] reported the formation of both chlorides during the reaction of copper with chlorine for temperatures between 150 and 750 °C. For chlorinations up to 250 °C they obtserved that copper reacts to form CuCl, which forms $CuCl_2$ by further reaction, leading to a layered morphology.

Interactions between reaction products and solid reactants during the chlorination of multi-component systems are known. [19,20] For that reason, similar behaviours are to be expected during the chlorination of alloys.

A gaseous complex between aluminium and copper chlorides, namely $CuAl_2Cl_8$, was obtained during a process of etching an aluminium–copper alloy. Its occurrence allows to convert copper chlorides to a form having sufficient volatility for removal by complexing with the aluminium chloride. The complex is readily detected in the gas phase at 280 °C [21]. A ΔG° value of 33.71 kJ/mol has been reported for the formation of the gaseous complex from solid $CuCl_2$ and gaseous Al_2Cl_6 [22].

* Corresponding author at: Centro Atómico Bariloche, Bustillo 9500, R84002AGP, S.C. de, Bariloche, Río Negro, Argentina.
E-mail address: demiccog@cab.cnea.gov.ar (G. De Micco).

0040-6031/$ – see front matter © 2007 Elsevier B.V. All rights reserved.
doi:10.1016/j.tca.2007.02.012

Finally, the Raman spectrum of the complex was measured by Emmenegger et al. for temperatures up to 300 °C. They found that on increasing temperature, the spectrum of $CuAl_2Cl_8(g)$ appears with increasing intensity [23].

In the present work, the chlorination of Al–Cu alloys was investigated for the first time. Following the reaction process it is possible to establish the general stages of the chlorination and to reveal the interactions that occur between the different compounds. The effect of temperature and alloy composition on chloride volatilization is analyzed.

2. Experimental details

2.1. Alloys

Commercial metals (99.9% purity) were used to prepare the following alloys: Al 46 wt.%–Cu, Al 18 wt.%–Cu and Cu 4 wt.%–Al. A powder of each alloy was prepared by mechanical abrasion with an analytical mill (IKA Labortechnik). Thermal treatments at 450 °C for 24 and 52 h in air were performed to release possible residual tensions. The powder samples of each alloy were well characterized by energy dispersive X-ray fluorescence (ED-XRF), scanning electron microscopy (SEM) and X-ray diffraction (XRD). The results are shown in Fig. 1.

As the figure shows, Al 46 wt.%–Cu and Al 18 wt.%–Cu are isotropic particles with faceted faces of different sizes from various microns to about 100 μm. Cu 4 wt.%–Al powder consists of needle-shped particles of about 1000 μm long. XRD patterns obtained show that the structures of the alloys are the intermetallic compound Al_2Cu for the Al 46 wt.%–Cu alloy, the gamma phase (Al_4Cu_9) for the Al 18 wt.%–Cu alloy, and a mixture of Al and Al_2Cu for the Cu 4 wt.%–Al alloy.

2.2. Chlorination

The gases used were Cl_2 99.8% purity (Indupa, Argentina) and Ar 99.99% purity (AGA, Argentina). Isothermal and non-isothermal chlorination reactions were carried out in a thermogravimetric analyzer (TGA), which is extensively described elsewhere [24]. This thermogravimetric analyzer consists of an electrobalance (Model 2000, Cahn Instruments, Inc.) suitable for working with corrosive atmospheres, a gas line and an acquisition system. This experimental set-up has a sensitivity of ±5 μg while operating at 950 °C under a flow of 8 l/h. Samples of 20 mg were placed in a quartz crucible inside the reactor in an argon flow of 1.3 l/h. To begin the non-isothermal reactions, a chlorine flow of 0.8 l/h was introduced and, at the same time, the heating started with a ramp of 100 °C/h. For the isothermal reactions, the solids were heated until they reached the desirable temperature before chlorine injection. The partial pressure of chlorine in the Ar–Cl_2 mixture was 35.5 kPa. Over the experimental conditions described above, the rate order of the alloy chlorinations is 10^{-6} mol of Cl_2/s, which reveals a gaseous phase diffusion control as demonstrated by previous publications [18,25]. Therefore, the influence of particle size in the reaction rate was considered negligible.

3. Results and discussion

3.1. Reactivity of Al–Cu alloys

The chlorination of the Al–Cu system was studied by focusing on the chlorination of three alloys. From the thermodynamic point of view, the negative ΔG° values for the chlorination of copper and aluminium [26] indicate that these reactions are thermodynamically feasible at all temperatures. However, it is well known that when a naked metal or alloy surface is put in contact with air, an oxide scale is formed, which depending on its microstructural characteristics will have different protective properties towards the corrosive agents. This is why it can be asserted that some metals will not react when they are put in direct contact with chlorine, until the conditions are appropriate for its penetration through the passivated oxide film and the contact of the gas with the underlying metal is made. Chlorine can reach the bulk metal by chlorination of the protective oxide scale or by diffusion through grain boundaries or through structural vacancies of the oxide film.

The ΔG° values for the chlorination reactions are negative for copper oxide, and positive for aluminium oxide, at temperatures below 1000 °C [26]. According to this, copper oxide will react while aluminium oxide will not. Therefore, in the case of copper, chlorine can reach the metal either by chlorination of the oxide scale or by diffusion through the scale depending on the relative velocities of the two mechanisms. On the other hand, aluminium will be attacked by chlorine only when diffusion of chlorine through the oxide scale takes place.

3.1.1. Non-isothermal chlorination of Al, Cu, Al 46 wt.%–Cu, Al 18 wt.%–Cu, and Cu 4 wt.%–Al

The initial reaction temperature which is associated with the system reactivity was determined by non-isothermal thermogravimetric measurements. The chlorination curves for each alloy together with the chlorination of the pure metals are shown in Fig. 2. This figure shows the ratio between the mass change and the initial mass of the sample as a function of temperature.

In Fig. 2, we can see that the starting temperatures for the reactions of the copper-rich and aluminium-rich alloys are similar to those of the corresponding pure metals, while the Al 46 wt.%–Cu alloy starts at a higher temperature.

For the Al 18 wt.%–Cu alloy, the reaction starts at about 100 °C, the same for copper. The chlorination of Cu 4 wt.%–Al starts at about 175 °C, and this temperature is 45 °C higher than the starting temperature for pure aluminium (130 °C). Besides, the mass changes observed in the chlorination of these alloys are in accordance with the mass changes observed in the chlorination of the constituents. The copper-rich alloy presents a mass gain and the same happens in the chlorination of copper due to the formation of condensed copper chlorides. The chlorination of the aluminium rich alloy shows a mass loss, also observed in the chlorination of aluminium due to the volatilization of aluminium chlorides.

The chlorination of the Al 46 wt.%–Cu alloy starts at 230 °C, while reactions of the pure metals start at 100 °C for copper and

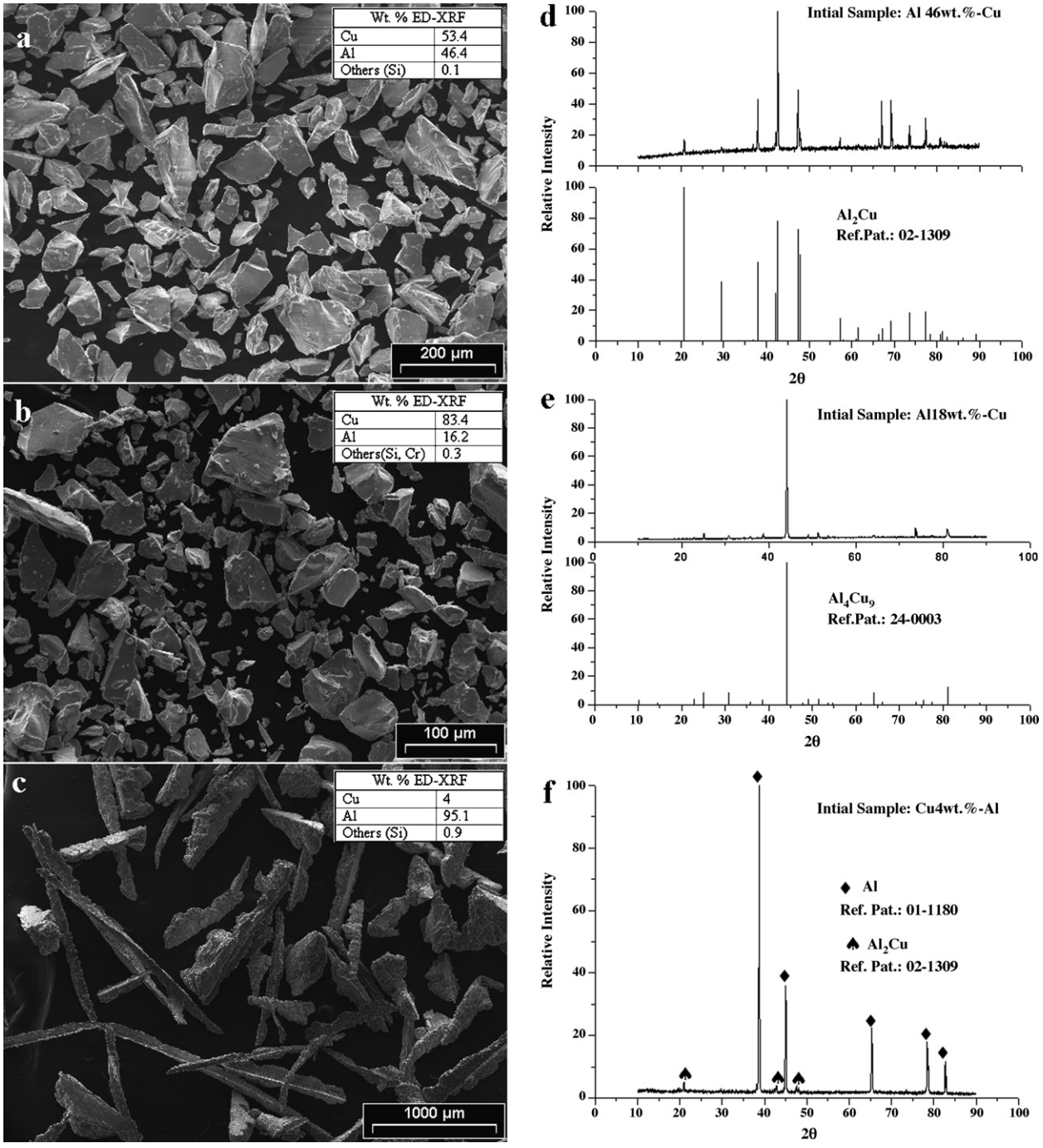

Fig. 1. Morphology, composition and structure of the initial samples: (a) and (d) correspond to powder of Al 46 wt.%–Cu alloy, (b) and (e) powder of Al 18 wt.%–Cu alloy, and (c) and (f) powder of Cu 4 wt.%–Al alloy. XRD reference patterns from Ref. [28].

at 130 °C for aluminium, as mentioned before. Moreover, the mass change observed in the alloy chlorination is very different from that of the pure metals. To investigate whether the constant mass observed in the first part of the curve, i.e. below 230 °C, is due to the absence of reaction or is the result of the compensation between condensed copper chlorides and gaseous aluminium chlorides, we did an isothermal chlorination at 200 °C for 2 h. In that experiment, no mass change was observed. Photographs of the initial and chlorinated samples obtained with SEM are also shown in Fig. 2a and b, respectively, and they reveal that there were no changes in the sample morphology. Finally, XRD analysis of the same sample confirmed that there was only Al_2Cu. This behaviour is different from that observed in the chlorination of the pure metals because both begin to react at 200 °C. The reactivity of the alloy at this temperature is thus lower than that of the pure metals.

3.2. Chlorination of Al 46 wt.%–Cu (Al_2Cu)

To study the general way in which the chlorination reactions of Al–Cu alloys take place, we analyzed in particular the chlorination of Al_2Cu.

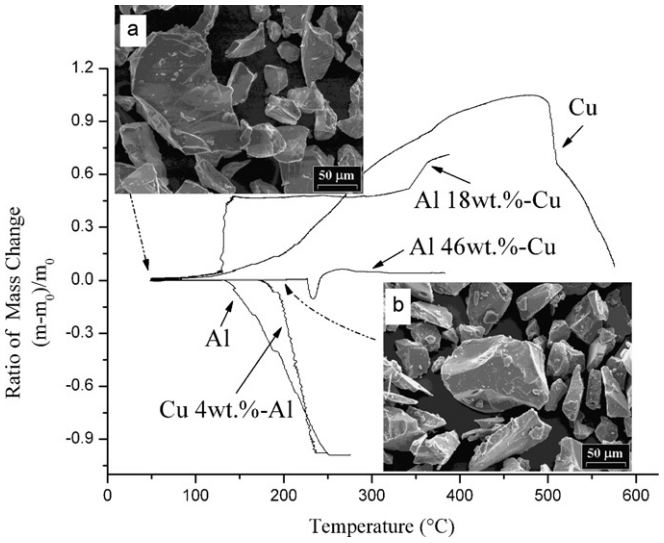

Fig. 2. Non-isothermal TG curves for the chlorination of Cu, Al, Al 46 wt.%–Cu, Al 18 wt.%–Cu, and Cu 4 wt.%–Al. (a) Initial sample for the chlorination of Al 46 wt.%–Cu, (b) unreacted Al 46 wt.%–Cu alloy after 2 h of chlorination at 200 °C.

As was reviewed by Chang and Wei [12], high temperature chlorine corrosion rate has two contributions: diffusion of ions through the chloride scale, when a layered product is formed, and volatilization of the scale. Therefore, typical curves of weight change vs. time for metals show a parabolic mass gain during the growth period of metal chloride if volatilization effect is not significant, followed by a linear mass loss when growth of chloride is not fast enough to supply the amount required for volatilization. Usually, diffusion of ions through the chloride scale is fast enough only at temperatures above 0.5 T_m, (T_m: melting point), and volatilization is significant only at vapour pressures above 10^{-2} kPa (10^{-4} atm). The values of T_m and T_4 (the temperature at which the vapour pressure is 10^{-4} atm) for copper and aluminium chlorides are presented in Table 1.

During copper chlorination reactions, formation of a product layer consisting of CuCl and $CuCl_2$ has been reported [18]. For temperatures below 275 °C (about 0.5 T_m for $CuCl_2$) this layer tends to stop the reaction by blocking ion diffusion. On the other hand, in the chlorination of aluminium, volatilization of $AlCl_3$ does not allow the formation of a protective scale.

The TG curve for the chlorination of Al_2Cu at 400 °C is shown in Fig. 3. The shape of this curve is entirely different from the typical mass changes versus time curves described before, which put in evidence that there are several simultaneous processes taking place. The reaction starts with a mass loss

Table 1
Aluminium and copper chlorides melting point (T_m) and temperatures (T_4) at which the chloride vapour pressure is 10^{-2} kPa (10^{-4} atm)

Chloride	T_m (°C)	T_4 (°C)	Reference
$AlCl_3$	181 sublimates	75	[13,25]
CuCl	422	950	[14,25]
$CuCl_2$	500	Decomposes	[18]

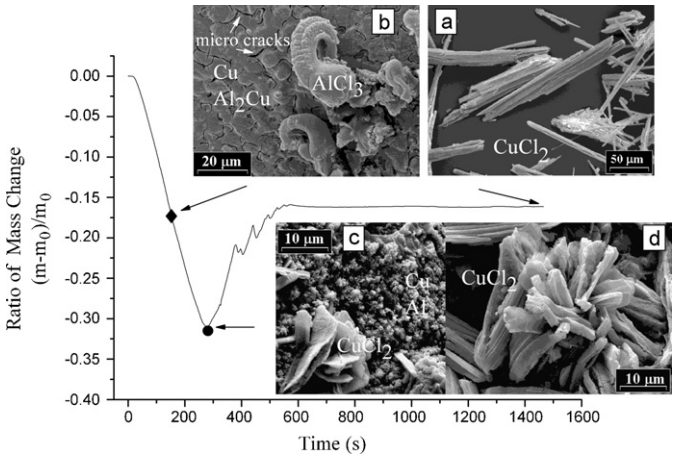

Fig. 3. Isothermal TG curve for the chlorination of Al 46 wt.%–Cu at 400 °C. (a) Reaction products, (b) reaction quenched during the mass loss, indicated by ♦, (c) and (d) reaction quenched in the minimum, indicated by ●.

followed by a mass gain, after which, the mass remains constant. We analyzed the chlorination residues that stayed in the crucible at the end of the reaction by different techniques. XRD patterns (Fig. 4a) showed the presence of only $CuCl_2$, ED-XRF and EDS analyses confirmed that the amounts of copper and chlorine correspond to $CuCl_2$, and a small amount of aluminium was also detected (between 0.5 and 2 wt.%). SEM examinations (Fig. 3a) showed a uniform morphology of needles already observed for $CuCl_2$ [27].

According to these results, during the chlorination reaction almost all aluminium forms volatile chlorides that evaporate. This can be explained since the vapour pressure of $AlCl_3$ is 10^{-2} kPa at 75 °C (see Table 1). However, there is also part of the initial copper that evaporates, as will be discussed subsequently. This is an unexpected result, taking into account that the vapour pressure of copper chlorides reaches a value of 10^{-2} kPa at temperatures considerably higher, as shown in Table 1.

In order to understand how the alloy chlorination occurs, we proceeded to interrupt the chlorination reactions at different

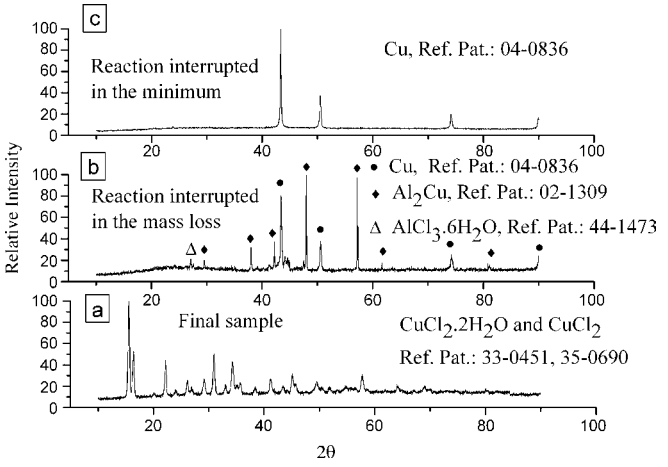

Fig. 4. XRD patterns obtained at different stages during the chlorination of Al 46 wt.%–Cu at 400 °C. XRD reference patterns from Ref. [28].

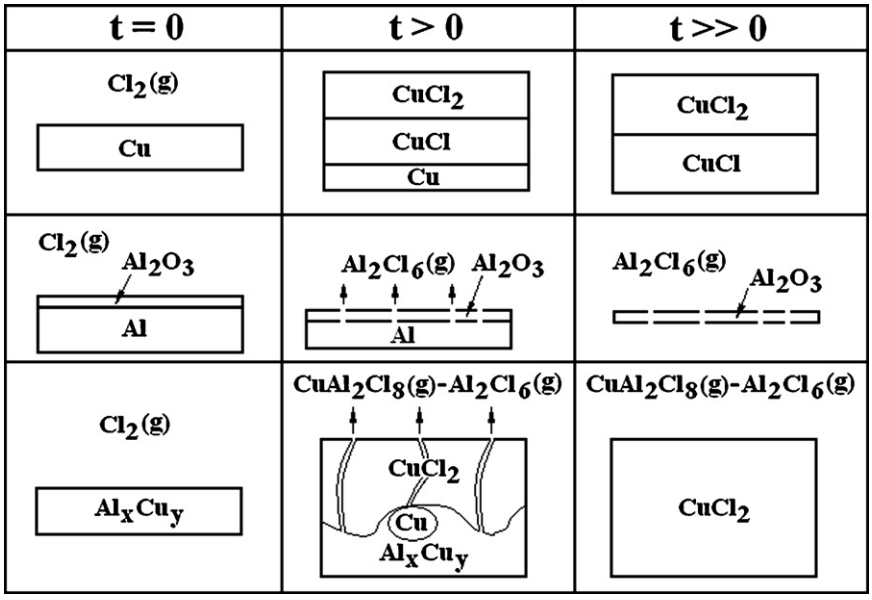

Fig. 5. Schematic diagram for the chlorination evolution of copper, aluminium and Al–Cu alloys.

reaction degrees (as shown by symbols in Fig. 3) and to analyze the samples by XRD and SEM. SEM photographs obtained are shown in Fig. 3(b–d), and XRD patterns are presented in Fig. 4. In the first part of the curve during the mass loss, XRD patterns (Fig. 4b) show that there is Al_2Cu, Cu and small peaks that may correspond to $AlCl_3{\cdot}6H_2O$. The presence of remaining $AlCl_3$ can be understood considering that the sample was quenched before the chlorination is completed. Due to the fast temperature decrease, part of the $AlCl_3$ which is being formed, is not able to volatilize and remains with the solid product. The occurrence of metallic copper means that aluminium is being eliminated faster than copper by volatilization of its chloride. However, copper chlorination does occur as well during the first part of the reactions, the presence of $CuCl_2$ was confirmed by interrupting and quenching several partially chlorinated samples at different temperatures. SEM micrographs (Fig. 3b) also reveal that the reaction proceeds through the formation of micro cracks in the solid alloy, and the aluminium chloride formed escapes from those cracks.

At the minimum of the curve, the morphology of the sample is completely different (Fig. 3c) there is a sintering powder of metallic copper with a small content of aluminium (about 12 wt.%, according to EDS measurements), and there are also some $CuCl_2$ crystals. XRD profile shows mainly copper (Fig. 4c).

A curious feature of this curve is the fluctuations observed between 400 and 600 s. This behaviour may be due to the formation of condensed chlorides (mainly from copper) that stop the reaction by preventing chlorine to contact the remaining metal, at the point where the rate of mass gain reaches a zero value, the volatilization rate becomes clear. After some seconds of mass loss, the chloride layer thins and allows chlorine to reach fresh metal, leading again to a subsequent mass gain.

A schematic diagram for the reaction of copper, aluminium and Al–Cu alloys is presented in Fig. 5.

3.3. Influence of temperature in the chlorination of Al–Cu alloys

We did isothermal chlorinations of the different alloys in the range between 175 and 500 °C, and chlorine partial pressure of 35.5 kPa. The influence of temperature on the chlorination reactions can be observed in Fig. 6 where the TG curves are presented.

The aluminium rich alloys (Fig. 6a) show a mass loss during the whole reaction which corresponds to volatilization of the chlorides formed. As Fig. 6a also shows, there is an initial time interval in which the mass loss rate is null or very slow. This time gap is smaller as temperature increases. Similar delays at the beginning of the reaction were observed in aluminium chlorination, especially for temperatures below 250 °C. The initial

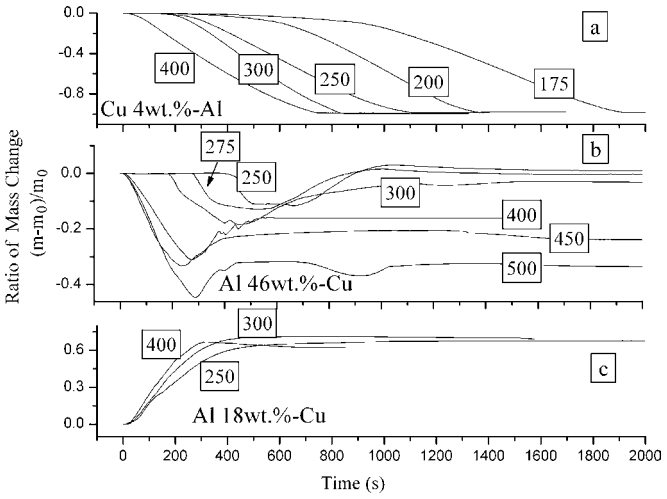

Fig. 6. Isothermal TG curves for the chlorination of (a) Cu 4 wt.%–Al between 175 and 400 °C, (b) Al 46 wt.%–Cu between 250 and 500 °C and (c) Al 18 wt.%–Cu between 250 and 400 °C.

time interval may correspond to an induction time due to the diffusion of chlorine through the oxide scale.

The total mass loss corresponds to about 98% of the initial mass of the sample. The difference is due to the non-reactive aluminium oxide scale and also to some copper chlorides as will be discussed in the next section.

The TG curves for the chlorination of Al 46 wt.%–Cu alloys are shown in Fig. 6b. Again, for temperatures below 400 °C, the reaction does not start immediately, as evidenced by an initial time span with no-mass-change. This behaviour is similar to that of aluminium, as mentioned before, and is different from that observed in the chlorination of copper powder for the same conditions of gaseous flow and partial pressure of chlorine. In that case, the mass gain starts immediately after chlorine reaches the metal for temperatures above 200 °C. Another characteristic of the TG curves that can be observed in Fig. 6b is that, as temperature increases, the initial mass loss is larger and the amount of the final sample is smaller. For temperatures above 500 °C, at the end of the curve the mass continuously decreases until complete volatilization, whereas for other temperatures the mass reaches an almost constant value. This is in agreement with the volatilization detected in copper chlorination reactions where a similar behaviour was observed [18]. Finally, in Fig. 6c the chlorination TG curves for the Al 18 wt.%–Cu alloy at three temperatures are presented. These reactions show a mass gain typical of condensed copper chloride formation. However, simultaneous evaporation of volatile chlorides does occur as evidenced by the low mass gain observed, and confirmed by analysis of the final condensed products, as will be discussed subsequently.

3.4. Reaction products from the chlorination of Cu and Al–Cu alloys

The chlorinated samples from the reaction of Al 46 wt.%–Cu and Al 18 wt.%–Cu were analyzed by XRD. We found that they consist of $CuCl_2$ for all temperatures, except for 500 °C (in the case of Al 46 wt.%–Cu) where CuCl was also detected. To avoid $CuCl_2$ decomposition after the reaction at the highest temperatures, i.e. at 450 and 500 °C, the samples were cooled in Cl_2 atmosphere [18].

The absence of CuCl at the lower temperatures is in accordance with thermodynamical data [26]. The ΔG° values for the reaction $2CuCl + Cl_2(g) \rightarrow 2CuCl_2$ are negative for temperatures up to about 400 °C where it has a value of −3.295 kJ/mol of Cl_2, indicating that the most stable specie is $CuCl_2$ below that temperature. However, in the reaction of pure copper powder with chlorine at 200 and 300 °C, we found that the chlorinated sample consisted of a mixture of CuCl and $CuCl_2$. The presence of CuCl in that case was attributed to a deficit of chlorine established by the formation of solid $CuCl_2$, which retards or prevents the contact between Cl_2 and CuCl [18]. In the alloy chlorination, a possible explanation for the absence of CuCl is that the continuous evaporation of $AlCl_3$ from the solid does not allow the formation of that protective layer of $CuCl_2$ and gives a path for chlorine to reach CuCl and form $CuCl_2$.

SEM analyses of the chlorinated samples allowed us to investigate the morphologies of the reaction products. Fig. 7a–e correspond to the samples after chlorination of copper at 300 °C, Al 18 wt.%–Cu at 250 °C, Al 46 wt.%–Cu at 400 °C, mixture of Al and Cu powders in the ratio of Al_2Cu at 400 °C, and Cu 4 wt.%–Al at 250 °C, respectively. Only one temperature is presented for each system because the morphologies of the final samples were essentially the same in the temperature range studied. As mentioned above, XRD of these samples indicated that they consist of $CuCl_2$ in the case of the alloy chlorination, whereas for copper chlorination CuCl was also detected.

SEM observations revealed that $CuCl_2$ grows in needles and, the morphology of the chlorides obtained in the chlorination of alloys, as well as in pure copper, is the same. However, the $CuCl_2$ crystal growth is more important during the chlorination of Al–Cu systems (Fig. 7b–e) than in the chlorination of pure copper (Fig. 7a).

The atomic percentage of aluminium contained in the copper chlorides was determined by ED-XRF and EDS for the different alloys, and the results are shown in Table 2. It can be seen that the values are below 5% and they seem not to be influenced by temperature or alloy composition. The amounts of aluminium contained in the final samples are attributed to the non-reactive aluminium oxide scale.

3.4.1. Enhanced volatilization of copper chlorides

It is possible to calculate the amount of chlorides evaporated during the chlorination reactions from the difference between the initial and final masses of each metal. To do that, we measured the final composition corresponding to the chlorination of Al 46 wt.%–Cu and Al 18 wt.%–Cu, and a mixture of Al and Cu powders in the ratio of Al_2Cu, at different temperatures with ED-XRF (the corresponding results for one temperature are shown also in Fig. 7f). The amount of the final samples after chlorination of Cu 4 wt.%–Al were not large enough to be measured by ED-XRF and, consequently, their compositions were analyzed by EDS.

In Table 3, the percentages of the initial mass of copper volatilized during the chlorination of Al–Cu systems compared with metallic copper [18] are shown. Taking into account that the volatilization of copper chlorides is negligible during the chlorination of pure copper (see Table 3), our results clearly show that the presence of aluminium enhances the volatilization of copper chlorides during the chlorination reactions. This enhancement can be understood by considering the formation of a gaseous complex between Al_2Cl_6 and $CuCl_2$, according to the following

Table 2
Percentage of aluminium in the final samples corresponding to the chlorination of different alloys at temperatures between 250 and 400 °C

Temperature (°C)	Percentage of aluminium in the final copper chlorides		
	Al 18 wt.%–Cu	Al 46 wt.%–Cu	Cu 4 wt.%–Al
250	1.6	2	4.5
300	2	1.4	
400	2	1	5

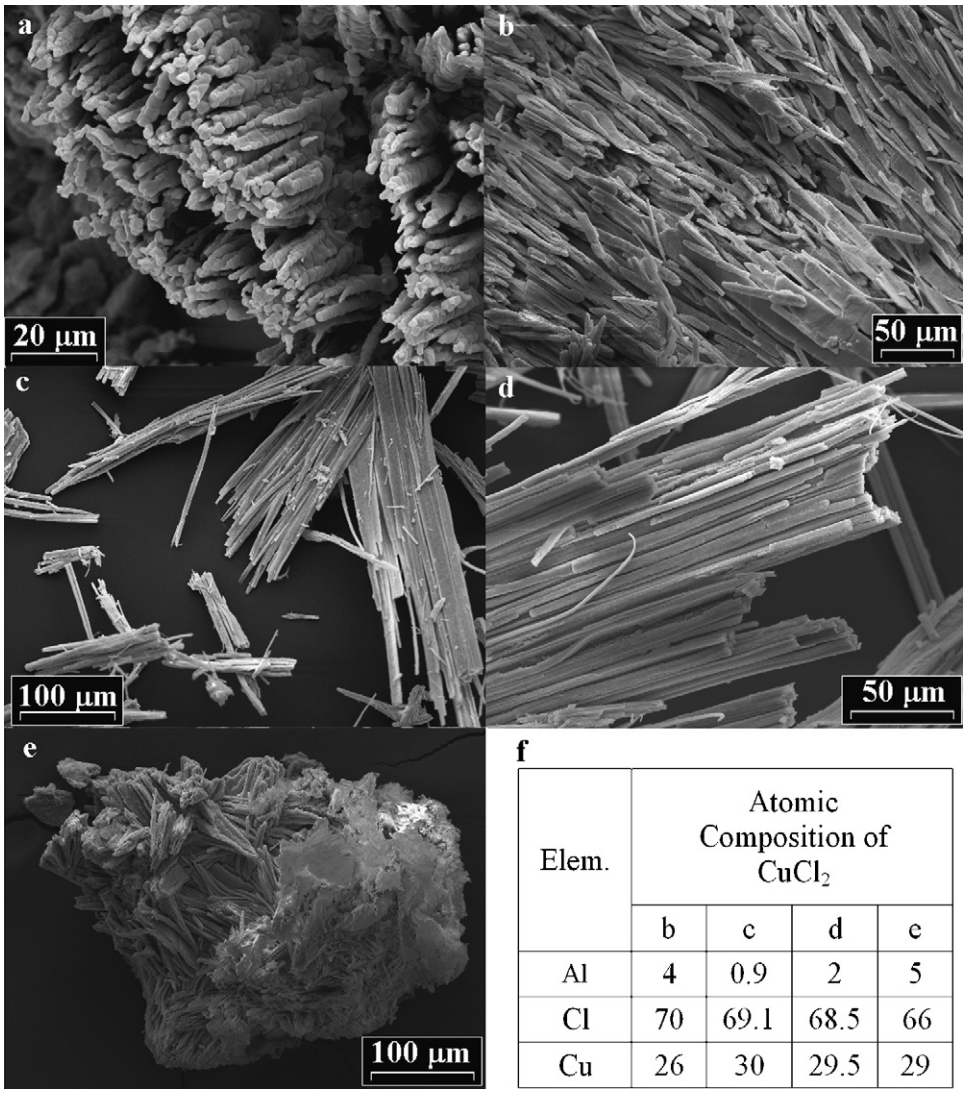

f

Elem.	Atomic Composition of $CuCl_2$			
	b	c	d	e
Al	4	0.9	2	5
Cl	70	69.1	68.5	66
Cu	26	30	29.5	29

Fig. 7. Final samples from the chlorination of: (a) copper at 300 °C, (b) Al 18 wt.%–Cu at 250 °C, (c) Al 46 wt.%–Cu at 400 °C, (d) mixture of Al and Cu powders in the ratio of Al_2Cu at 400 °C, (e) Cu 4 wt.%–Al at 250 °C and (f) atomic composition of the samples determined by EDS and ED-XRF.

reaction [23]:

$$CuCl_2(s) + Al_2Cl_6(g) = CuAl_2Cl_8(g) \quad (1)$$

The presence of a high concentration of copper in the gaseous phase as $CuAl_2Cl_8$, can explain the well defined crystals of $CuCl_2$ obtained, which are bigger than those observed in the chlorination of copper (see Fig. 7). These chlorides are probably being formed from an isotropic media through a volatilization–crystallization mechanism during the reactions.

With a simple calculation based on the moles of copper lost during each reaction, and considering that all copper is volatilized as $CuAl_2Cl_8$, it is possible to estimate the average partial pressure of the complex under the experimental conditions. For example, in the chlorination of Al 46 wt.%–Cu at

Table 3
Percentage of copper volatilized for different metals and alloys at different temperatures, and the corresponding quantity: $S_{Cu/2Al}$

T (°C)	Percentage of the initial mass of copper volatilized in the chlorination of different metals an alloys				Moles of Cu that were volatilized every two moles of Al volatilized ($S_{Cu/2Al}$)		
	Cu[a]	Al 18 wt.%–Cu	Al 46 wt.%–Cu	Cu 4 wt.%–Al	Al 18 wt.%–Cu	Al 46 wt.%–Cu	Cu 4 wt.%–Al
250	Non-detected	23	19	84	~1	0.19	0.03
300	Non-detected	22	22	100	0.98	0.22	0.03
400	<0.5	26	32 29[b]	95	~1	0.32 0.30[b]	0.03

[a] Ref. [18].
[b] Corresponds to the chlorination of a mixture of powders of copper and aluminium in the ratio of Al_2Cu.

400 °C, P($CuAl_2Cl_8$) is about 10^{-1} kPa (10^{-3} atm). The results obtained are in good agreement with the values of P($CuAl_2Cl_8$) calculated taking into account the ΔG° values for reaction (1) [22], P(Al_2Cl_6) 10^2 kPa (1 atm), and the same experimental conditions. Although the chlorinating gas is a mixture of Cl_2–Ar, in the sample surroundings $AlCl_3$ is being generated and Cl_2 is being exhausted by the reaction, for that reason the partial pressure of $AlCl_3$ is expected to be high. Moreover, the residence time of $AlCl_3$ in the sample is long due to the low gaseous flow (2.1 l/h) and because the $AlCl_3$ formed has to diffuse through a $CuCl_2$ layer before reaching the gaseous phase, as schematically shown in Fig. 5.

To compare the behaviour of the different Al–Cu systems, it is useful to calculate the moles of copper that are volatilized for every 2 mol of aluminium during each chlorination reaction:

$$s_{Cu/2Al} = \frac{\text{(moles of Cu volatilized during the chlorination)}}{2 \times \text{(moles of Al volatilized during the chlorination)}}$$

This quantity is called $S_{Cu/2Al}$ and is also shown in Table 3. Therefore, taking into account Eq. (1), $S_{Cu/2Al} \sim 1$ means that all aluminium that left the sample has formed $CuAl_2Cl_8$. On the other hand, low values of $S_{Cu/2Al}$ ($S_{Cu/2Al} \sim 0$) indicate that most of the aluminium left the sample as Al_2Cl_6 without forming the gaseous complex.

When moving from left to right in Table 3, due to an increase in the relative content of aluminium in the alloys, an increase in the partial pressure of Al_2Cl_6 is expected. Meanwhile, owing to the lower percentages of copper in the alloys which lead to the formation of less $CuCl_2$, there would be a decrease in the surface of reaction for the formation of the gaseous complex.

Therefore, the $S_{Cu/2Al}$ values obtained for each alloy may give evidence on which of the above mentioned opposite behaviours is determining the amounts of complex formed. In the Al 18 wt.%–Cu alloy, the value of $S_{Cu/2Al} \sim 1$ indicates that all the aluminium chloride available is forming $CuAl_2Cl_8$ and this is expected since Al_2Cl_6 is the limiting reactant considering the reaction given by Eq. (1) and the alloy composition. On the other hand, for the Al 46 wt.%–Cu alloy, which has the same Cu/Al ratio of the complex, the low values of $S_{Cu/2Al}$ give evidence that, in this case, $CuCl_2$ is the limiting specie in the complex formation reaction. According to these results, the maximum partial pressure of $AlCu_2Cl_8$ would occur at some intermediate alloy composition between Al 46 wt.%–Cu and Al 18 wt.%–Cu. The aluminium content of alloy has to be as high as possible to produce the maximum Al_2Cl_6 partial pressure in combination with a high reaction surface, i.e. enough amount of $CuCl_2$ available for the reaction.

Finally, for the Cu 4 wt.%–Al alloy, the initial amount of copper is below the stoichiometric quantities of the complex, copper being the limiting reactant in this case. The surface of interaction between $CuCl_2$ and Al_2Cl_6 is significantly reduced, leading to a very low partial pressure of $CuAl_2Cl_8$, as can be seen from the values of $S_{Cu/2Al} \sim 0$. The high percentage of initial mass of copper volatilized for this alloy are not related with a great amount of complex formed, but are due to the initial composition of alloy which has a small amount of copper. For this alloy even a low partial pressure of the complex represents a high portion of the initial mass of copper.

Regarding the effect of temperature, the partial pressure of the complex increases with temperature, as can be seen in Table 3 were there is a slight increase in the percentage of copper chlorides being volatilized with temperature. This is to be expected since the reaction given by Eq. (1) is endothermic [23]. Furthermore, as is also shown in Table 3, the volatilization is the same for the case of the Al 46 wt.%–Cu alloy chlorination and for the mixed powders of pure metals. This indicates that the only interactions which are important in the complex formation are those between gaseous aluminium chloride and the surface of solid $CuCl_2$.

4. Conclusions

The initial temperature for the reaction of selected Al–Cu alloys with chlorine was experimentally determined. For the Al 18 wt.%–Cu and Cu 4 wt.%–Al alloys, the behaviour observed was similar to that of pure copper and aluminium, respectively. On the other hand, for the Al 46 wt.%–Cu alloy, a significant increase in the reaction temperature was found, which can be due to a change in the microstructure of the oxide scale.

The chlorination of Al 46 wt.%–Cu at 400 °C was analyzed in detail. We found that $CuCl_2$ is the only solid product. At intermediate stages of the reaction, we detected metallic copper which indicates that aluminium is being removed from the alloy by the volatilization of its chloride faster than copper.

The needle morphology of the $CuCl_2$ obtained in the chlorination of alloys is the same that was observed in copper chlorination reactions. However, in the case of the alloys, the crystals are much bigger. This was attributed to the high partial pressure of $CuAl_2Cl_8$ which would lead to a volatilization–crystallization growth mechanism during the reaction.

Finally, regarding chloride interactions, we found that volatilization of copper chlorides is enhanced during the alloy chlorination. The volatilization observed for the different alloys can be understood taking into account the $CuAl_2Cl_8$ formation reaction which involves solid $CuCl_2$ reacting with gaseous Al_2Cl_6.

Acknowledgements

The authors would like to thanks the Agencia Nacional de Promoción Científica y Tecnológica (ANPCyT), Consejo Nacional de Investigaciones Científicas y Técnicas (CONICET) and Universidad Nacional del Comahue for the financial support of this work.

References

[1] R.L. De Beauchamp, Preparation of Anhydrous Aluminium Chloride, Inf. Circ. U.S. Bur. Mines, no 8412, 1969.
[2] C. Furnas (Ed.), Roger's Industrial Chemistry, vol. 1, Van Nostrand, New York, 1942, p. 460 (ch. 2).
[3] Synthesis of Aluminium Chloride. Report from the internet: http://www.rhodium.ws.

[4] L.S. Belknap, Aluminum trichloride production, US Pat. 3,721,731, Cabot Corporation, Boston, Massachusetts, USA, 1973.
[5] L. Piccolo, M. Ghirga, B. Calcagno, Process for preparing aluminium trichloride, US Pat. 3,812,241, Societa Italiana Resine S.I.R.S.P.A., Milan, Italy, 1974.
[6] J.P. Remeika, B. Batlogg, Mater. Res. Bull. 15 (1980) 1179–1182.
[7] N. Bourhila, N. Thomas, J. Palleau, J. Torres, C. Bernard, R. Madar, Appl. Surf. Sci. 91 (1995) 175–181.
[8] I. Gaballah, M. Djona, J.C. Mugica, R. Solozabal, Resour. Conserv. Recycling 10 (1–2) (1994) 87–96.
[9] R.E. Siemens, B.W. Jong, J.H. Russell, Conserv. Recycling 9 (2) (1986) 189–196.
[10] K. Matsumaru, M. Susa, K. Nagata, J. Iron Steel Inst. Jpn. 82 (10) (1996) 1–6.
[11] A. Landsberg, J. Less-Common Met. 159 (1990) 163–172.
[12] Y.N. Chang, F.I. Wei, J. Mater. Sci. 26 (1991) 3693–3698.
[13] O. Helmboldt, L. Keith Hudson, C. Misra, K. Wefers, H. Stark, M. Danner, Ullman's Encyclopedia of Industrial Chemistry, sixth ed., Electronic Release. Aluminium Compounds, Inorganic-Aluminium Chloride, 2002.
[14] H. Wayne Richardson, Ullman's Encyclopedia of Industrial Chemistry, sixth ed., Electronic Release. Copper Compounds—Salts and Basic Salts, 2002.
[15] R. Titi-Manyaka, I. Iwasaki, Trans. SME/AIME 260 (1976) 282–288.
[16] W. Sesselmann, T.J. Chuang, Surf. Sci. 176 (1986) 32–66.
[17] W. Sesselmann, T.J. Chuang, Surf. Sci. 176 (1986) 67–90.
[18] G. De Micco, A.E. Bohé, D.M. Pasquevich, J. Alloys Compd., in press doi:10.1016/j.jallcom.2006.08.
[19] J.A. González, F.C. Gennari, M. del Carmen Ruiz, A.E. Bohé, D.M. Pasquevich, Trans. Inst. Min. Met. Section C 107 (1998) 130–138.
[20] A.E. Bohé, J.J. Andrade Gamboa, D.M. Pasquevich, Mater. Sci. Technol. 13 (1997) 865–871.
[21] N.J. Norvell, Process for etching an aluminium–copper alloy, U.S. Patent 4,468,284, http://www.freepatentsonline.com/4468284.html.
[22] A. Dell'Anna, F.P. Emmenegger, Helv. Chim. Acta 58 (1975) 1145.
[23] F.P. Emmenegger, C. Rohrbasser, W. Schläpfer, Inorg. Nucl. Chem. Lett. 12 (1976) 127–131.
[24] D.M. Pasquevich, A.M. Caneiro, Thermochim. Acta 156 (2) (1989) 275–283.
[25] F.C. Gennari, D.M. Pasquevich, Thermochim. Acta 284 (1996) 325–339.
[26] A. Roine, Outokumpu HSC chemistry for Windows, in: 93001-ORGT Version 2. 0, Outokumpu Research Oy Information Service, 1994.
[27] F.J. Alvarez, G. De Micco, A.E. Bohé, D.M. Pasquevich, IAEA. Technical Cooperation Regional Project, RLA/4/018, Final Report, March 2005.
[28] Joint Committee for Powder Diffraction Standards, International Center for Diffraction Data. Powder Diffraction File, 2001.